

# New Cardiac Imaging Algorithms to Diagnose Constrictive Pericarditis Versus Restrictive Cardiomyopathy

Ahmad Mahmoud<sup>1</sup> · Manish Bansal<sup>2</sup> · Partho P. Sengupta<sup>3</sup>

Published online: 12 April 2017  
© Springer Science+Business Media New York 2017

## Abstract

**Purpose of Review** Echocardiography is the mainstay in the diagnostic evaluation of constrictive pericarditis (CP) and restrictive cardiomyopathy (RCM), but no single echocardiographic parameter is sufficiently robust to accurately distinguish between the two conditions. The present review summarizes the recent advances in echocardiography that promise to improve its diagnostic performance for this purpose. The role of other imaging modalities such as cardiac computed tomography, magnetic resonance imaging, and invasive hemodynamic assessment in the overall diagnostic approach is also discussed briefly.

**Recent Findings** A recent study has demonstrated improved diagnostic accuracy of echocardiography with integration of multiple conventional echocardiographic parameters into a step-wise algorithm. Concurrently, the studies using speckle-tracking echocardiography have revealed distinct and disparate patterns of myocardial mechanical abnormalities in CP and RCM with their ability to distinguish between the two conditions. The incorporation of machine-learning algorithms into echocardiography workflow permits easy integration of the wealth of the diagnostic data available and promises to further enhance the diagnostic accuracy of echocardiography.

**Summary** New imaging algorithms are continuously being evolved to permit accurate distinction between CP and RCM. Further research is needed to validate the accuracy of these newer algorithms and to define their place in the overall diagnostic approach for this purpose.

**Keywords** Speckle tracking echocardiography · Myocardial deformation imaging · Machine-learning

## Introduction

Constrictive pericarditis (CP) and restrictive cardiomyopathy (RCM) have overlapping hemodynamic profiles and share a common clinical presentation of heart failure with preserved ejection fraction. The similarities in their hemodynamic profiles make the distinction between the two entities very challenging. However, this distinction is critical as the therapeutic options and the clinical outcomes of CP and RCM differ considerably. Whereas CP is a curable form of heart failure, RCM has only limited therapeutic options and is usually associated with a dismal prognosis.

Echocardiography is the imaging modality of choice for diagnostic evaluation of CP and RCM, both because of its ability to permit comprehensive morpho-functional assessment of the heart and its easy availability and safety. While echocardiography is generally sufficient to establish the correct diagnosis in most patients, overlapping findings between CP and RCM preclude accurate assessment in many patients. The advent of newer imaging modalities such as speckle tracking echocardiography (STE) with the development of newer analysis and interpretation algorithms have enhanced the diagnostic accuracy of echocardiography for this purpose. When the uncertainty still persists, cardiac computed tomography (CT), cardiac magnetic resonance (CMR), or even

This article is part of the Topical Collection on *Pericardial Disease*

✉ Partho P. Sengupta  
Partho.Sengupta@wvumedicine.org

<sup>1</sup> Department of Cardiovascular Medicine, Ain Shams University, Cairo, Egypt

<sup>2</sup> Heart Institute - Division of Cardiology, Medanta- The Medicity, Gurgaon, India

<sup>3</sup> Heart and Vascular Institute, West Virginia University, 1 Medical Center Drive, Morgantown, WV 26506, USA

invasive cardiac catheterization may be needed to aid in the diagnostic assessment.

## Echocardiography for Distinguishing between CP and RCM

### Conventional Echocardiographic Findings

Although the hemodynamic profiles of CP and RCM resemble each other, the underlying pathology in the two conditions is vastly different. Whereas external constraint due to encasement of the heart by the thickened, fibrotic, and often calcified pericardium is the underlying abnormality in CP, reduced myocardial compliance caused by abnormal elastic properties, which can be of primary origin or secondary to infiltrative diseases, is the dominant pathology in RCM. These pathogenic differences account for certain characteristic echocardiographic features that separate the two conditions. The pericardial constraint in CP results in marked ventricular interdependence, which is lacking in RCM. Additionally, unlike in the normal individuals and those with RCM, respiratory changes in intrathoracic pressure fail to get transmitted to inside the heart in CP. The echocardiographic distinction between CP and RCM predominantly relies on recognizing these key functional differences between the two entities (Table 1) [1<sup>••</sup>, 2<sup>••</sup>, 3<sup>••</sup>].

### Features of Ventricular Interdependence

As the total cardiac volume is fixed in CP, any increase in the volume and flow on one side of the heart must be accompanied by a concomitant reduction in the same on the other side. At the same time, decreased transmission of intrathoracic pressures to the heart with normal pressure transmission to the pulmonary veins leads to exaggerated pressure changes between the left atrium and the pulmonary veins, thereby further augmenting the influence of respiration on intracardiac filling. These phasic variations in right and left heart filling can be recognized in the form of several echocardiographic features, as described below.

**Abnormal Ventricular Septal Motion** In CP, the interventricular septum is shifted to the left during inspiration and to the right during expiration (Fig. 1). Although this respirophasic ventricular septal shift can be easily appreciated on two-dimensional (2D) echocardiography, M-mode permits a more accurate assessment due to its superior temporal resolution. The presence of ventricular septal shift is reported to be one of the most sensitive (93%) echocardiographic features of CP [4<sup>•</sup>]. However, severe obstructive lung disease or other conditions associated with increased respiratory effort may also lead to similar ventricular septal motion with respiration.

In addition to the respirophasic changes in septal position, the ventricular septum in CP also exhibits oscillatory motions during each cardiac cycle, termed as “septal shudder” or “septal bounce” (Fig. 1) [5–7]. This abnormal septal movement results from the combined influences of ventricular interdependence and temporal differences in left and right ventricular filling. M-mode echocardiography provides best visualization of the septal shudder which appears as a downward septal notch during early diastole followed by further, rapid, to- and fro- movements. Recently, tissue Doppler imaging (TDI), using both pulsed-wave (PW) and color TDI, has been shown to have better accuracy for recognition of this abnormal septal motion [8, 9]. However, it should be noted that abnormal septal motion is not specific for CP and can be present in other conditions also, such as intraventricular conduction abnormalities and post-cardiac surgery state [5, 10, 11].

Pericardial constraint in CP also results in a characteristic diastolic flattening of the posterior wall of the left ventricle which can be recognized on M-mode echocardiography [6, 12].

**Respiratory Variation in Intracardiac Flows** In CP, mitral inflow is reduced whereas tricuspid inflow is augmented during inspiration, with opposite changes occurring during expiration (Fig. 2). A ≥25% increase in the transmural early diastolic (E) velocity during inspiration and a ≥40% increase in the tricuspid inflow E velocity during expiration are highly suggestive of CP [3<sup>••</sup>, 13, 14]. Mitral E velocity deceleration time is also shortened during inspiration signifying rapidity of left atrial (LA) and left ventricular (LV) pressure equalization. The respiratory variation may be more consistently observed in pulmonary venous flow with an 18% or greater increase in pulmonary venous diastolic velocity during expiration being suggestive of CP [15]. However, it should be noted that respiratory variation in the mitral inflow velocities may not be present in about one third of the cases, esp. in overly diuresed or fluid-loaded patients [13, 16, 17]. Therefore, its absence does not exclude CP.

Although the patients with RCM may also demonstrate respiratory variation in mitral and tricuspid inflows, these changes are only modest but may occur in the presence of a pericardial effusion. Respiratory variation may also be present in several other conditions such as obstructive airway disease, sleep apnea, etc. [18]. However, in CP, the changes in flow velocities become apparent within the first beat during inspiration or expiration whereas the changes in respiratory diseases are more gradual. Further, respiratory diseases are characterized by marked inspiratory increase in superior vena cava flow, which is not seen in CP [19].

**Hepatic Vein Flow Velocities** In CP, rightward deviation of ventricular septum during expiration reduces hepatic vein

**Table 1** Sensitivity and specificity of various echocardiographic parameters for diagnosing constrictive pericarditis

Echocardiographic parameter	Sensitivity	Specificity
A combination of significant respiratory variation in peak early diastolic mitral inflow velocity and augmented hepatic vein diastolic flow reversal after the onset of expiration	88	67
Color M-mode mitral inflow propagation velocity $\geq 100$ cm/s	74	91
Pulmonary vein flow velocity		
Pulmonary vein systolic/ diastolic flow ratio $\geq 65\%$ in inspiration + % change in peak diastolic flow $\geq 40\%$	86	94
Respiratory variation in pulmonary vein peak diastolic flow velocity $\geq 18\%$	79	91
Hepatic vein diastolic reversal velocity/forward velocity in expiration $\geq 0.79$	76	88
Interventricular septal shift with respiration	93	69
Interventricular septal bounce		
M-mode	40–88	80
2D	62	93
Color TDI (biphasic early diastolic interventricular septal motion $\geq 7$ cm/s)	82	93
Pulsed-wave TDI	100	100
Left ventricular posterior wall flattening, M-mode	64–92	82–100
Pericardial thickening		
M-mode	53–100	50–100
2D	36	-
Mitral annular velocities on TDI		
Medial e' velocity $\geq 9$ cm/s	83	81
Medial and lateral e' velocity both $> 8$ cm/s	89	73
Medial e'/lateral e' $\geq 0.91$	75	85

Modified from: Dal-Bianco JP et al. J Am Soc Echocardiogr 2009;22:24–33, with permission from Elsevier) [1••]  
2D two-dimensional, e' early diastolic mitral annular velocity, TDI tissue Doppler imaging

forward velocity and exaggerates the late diastolic reversal velocity. In contrast, in RCM, diastolic filling on the right side is not compromised during expiration and there

are large reversals with inspiration and expiration. In a recent study, Welch et al. demonstrated that the ratio of the diastolic reversal flow velocity and the diastolic forward flow velocity during expiration could be useful for distinguishing between CP and RCM [4•]. A cutoff value of  $\geq 0.79$  for this ratio was found to have 76% sensitivity and 88% specificity for this purpose.

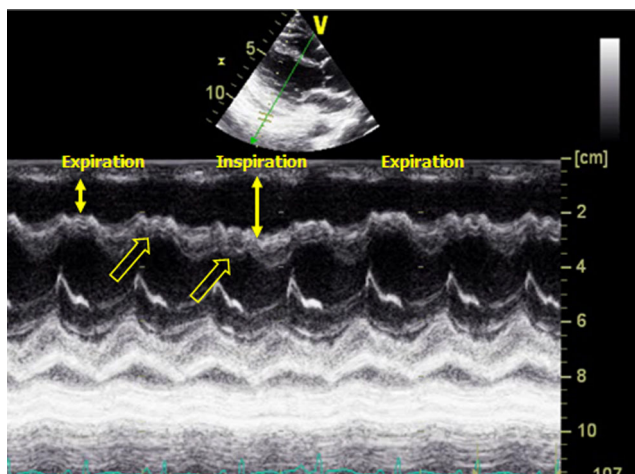


**Fig. 1** Abnormal ventricular septal motion in a patient with constrictive pericarditis. The septum moves towards the right ventricle during expiration and towards the left ventricle during inspiration (double-headed arrows). Additionally, there is a brisk oscillatory movement of the septum during diastole in each cardiac cycle, known as “septal shudder” (open arrows)

### Tissue Doppler Imaging

Pericardial constraint in CP limits radial expansion of the ventricles and therefore most of the diastolic filling occurs by means of longitudinal expansion. Moreover, as there is no impediment to ventricular filling during early diastole, early diastolic velocities are exaggerated. This is represented in the form of increased, or at least preserved, early diastolic medial mitral annular velocity (e') [15, 20–22]. In contrast, mitral e' velocity is invariably reduced in patients with RCM because of underlying myocardial dysfunction (Fig. 2). Several studies have demonstrated that medial e' velocity  $\geq 8$  cm/s is highly accurate in distinguishing between CP and RCM [15, 20–22]. A medial e' velocity  $\geq 9$  cm/s has been reported to have 83% sensitivity and 81% specificity for diagnosing CP [4•].

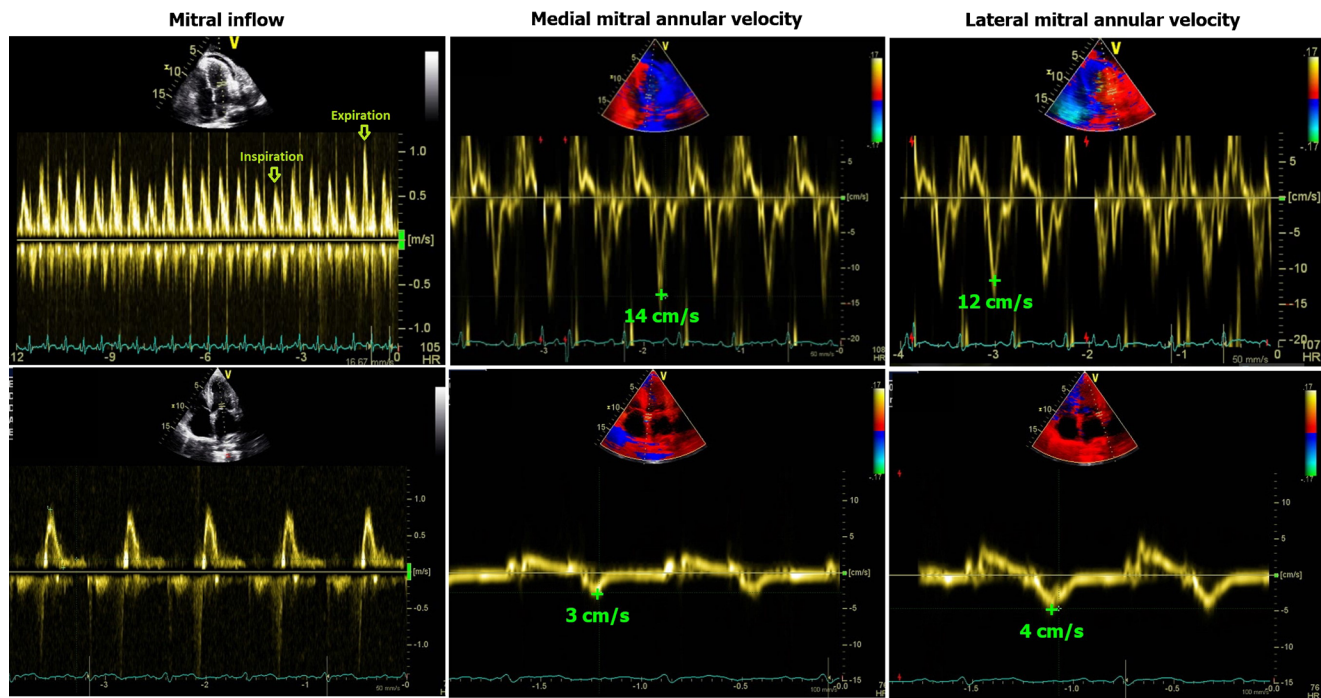


**Fig. 2** Significant respiratory variation in mitral inflow velocities with annulus paradoxus and annulus inversus in constrictive pericarditis (upper panel). In contrast, an opposite pattern is seen in restrictive cardiomyopathy (lower panel)

However, the presence of associated annular calcification and/or LV systolic dysfunction in cases of CP would compromise the diagnostic value of mitral  $e'$  [23].

The preserved or increased mitral annular  $e'$  velocity in CP also leads to a paradoxically low mitral  $E/e'$  velocity ratio, despite significantly elevated LV filling pressure. This is termed as “annulus paradoxus” (Fig. 2) [3••, 18, 24]. However, the diagnostic value of annulus paradoxus has been contested in recent studies [25].

An additional finding observed in CP is the reversed relationship between medial and lateral mitral annular  $e'$  velocities. In normal individuals, lateral  $e'$  is greater than medial  $e'$  due to greater excursion of the LV lateral wall as compared to the medial annulus which is relatively tethered. In CP, however, this relationship is reversed due to tethering of LV free wall by pericardial adhesions (Fig. 2). This finding, termed as “annulus inversus” was first described by Reuss et al. [26] and has been confirmed in several subsequent studies [4•, 27]. In the above-mentioned study by Welch et al., the ratio of medial  $e'/$ lateral  $e' \geq 0.91$  was found to have 75% sensitivity and 85% specificity for diagnosing CP, though it was not independently associated with CP on multivariate analysis [4•]. Similar to lateral mitral  $e'$ , some investigators have also reported reduced lateral tricuspid  $e'$  in CP [28].

Pericardectomy rapidly corrects the abnormalities of mitral annular motion. Medial mitral  $e'$  decreases soon after the surgery with normalization of the ratio of medial to lateral  $e'$  [27, 29•].

### Other Findings

Rapid, unimpeded early diastolic LV filling can also be appreciated on color M-mode of mitral inflow. Mitral inflow propagation velocity is typically  $>100$  cm/s in CP whereas it is markedly reduced in RCM [15]. A cutoff value of 45 cm/s provides good distinction but is technically more difficult to obtain than mitral annular velocities on TDI [30].

Pericardial thickening, with or without calcification, can be detected by echocardiography in the majority of the patients with CP. Transesophageal echocardiography (TEE) is more sensitive than transthoracic echocardiography for this purpose. A pericardial thickness of  $>3$  mm is very specific for CP, especially when seen together with septal bounce [18, 31]. However, absence of pericardial thickening does not exclude CP as pericardial thickness is reported to be normal in roughly 20% patients undergoing pericardectomy for CP [32]. Pericardial calcification is less common, seen only in 20–40% patients with CP and mostly in those with tubercular etiology [33].

Pericardial thickening also leads to tethering of RV free wall which can be appreciated on subcostal imaging [4•]. The movement of RV free wall at its interface with the liver appears restricted in CP, as compared to the free sliding motion seen normally. Additionally, pericardial thickening and calcification can lead to distortion of LV or RV contours. Although, this feature is found only in approximately one third of patients with CP, but when present, it is virtually diagnostic of CP [4•].

### *Integrating Conventional Echocardiographic Features for Differentiating CP from RCM*

While the earlier studies had demonstrated utility of individual echocardiographic parameters for distinguishing between CP and RCM, their hierarchical significance was not studied. To address this, Welch et al. compared diagnostic accuracies of various conventional echocardiographic features in 130 patients with surgically confirmed CP and 36 patients with either RCM or severe tricuspid regurgitation [40]. Three parameters were found to be independently associated with CP: respiratory shift in ventricular septal position, preserved ( $\geq 9$  cm/s) medial mitral e', and increased hepatic vein expiratory diastolic reversal ratio ( $\geq 0.79$ ). Ventricular septal shift had highest sensitivity (93%) to diagnose CP, and when combined with either preserved medial e' or exaggerated hepatic vein expiratory diastolic reversal ratio, it yielded a desirable combination of sensitivity (87%) and specificity (91%). The specificity increased to 97% when all three factors were present, but the sensitivity decreased to 64%. Based on these observations, a step-wise algorithm has been proposed for distinguishing between CP and RCM ("the Mayo Clinic criteria") [23]. Further studies are needed to validate the Mayo Clinic criteria.

### **Role of Myocardial Mechanics in Distinguishing between CP and RCM**

The advent of STE, with its ability to permit comprehensive assessment of myocardial mechanics, has allowed unique insights into the pathogenesis of various cardiac disorders, including CP and RCM [34••].

The LV myocardium is composed of muscle layers with helically oriented muscle fibers. This helical arrangement is responsible for the multidimensional deformation of the left ventricle. Although the LV myocardium behaves as a functional continuum, different muscle layers contribute to different components of LV deformation based on their spatial orientation with respect to the overall LV geometry. Subendocardial fibers, being more parallel to the long-axis of the left ventricle, determine mainly the longitudinal deformation of the left ventricle, whereas the subepicardial fibers which are more obliquely arranged are mainly responsible for the circumferential shortening and the rotational mechanics of the left ventricle [35–39]. Most of the myocardial diseases first affect the subendocardial region and therefore result in impairment of longitudinal deformation, while LV circumferential deformation and twist remain relatively preserved, at least during the initial stages [35, 39–41]. In contrast, the pericardial diseases initially affect the subepicardial myofibrils because of close anatomic proximity and therefore mostly affect the torsion and the circumferential shortening of the myocardium [29•, 35, 41, 42]. Additionally, pericardial adhesions may limit the free motion of the ventricle within the

pericardium and thereby also reduce LV twist directly. The same mechanism may also be responsible for reduction of the longitudinal motion of the free wall of the left ventricle [29•, 43, 44•]. This differential impairment of myocardial mechanics in CP and RCM has been shown to be diagnostically useful, as discussed below (Fig. 3).

### *Long-Axis Deformation in CP and RCM*

Consistent with the above observations, numerous studies have demonstrated reduced global longitudinal strain (GLS, average longitudinal strain of all LV segments) in patients with RCM [29•, 39, 41, 44•]. The reduction in longitudinal strain (LS) in these patients is generally uniform, affecting the whole left ventricle. However, in some forms of RCM, apical segments may be spared. Such apical sparing is a characteristic finding in cardiac amyloidosis [45, 46].

In contrast, the impact of CP on longitudinal deformation is variable, depending on the extent of pericardial tethering and the underlying myocardial dysfunction [29•, 44•, 47, 48]. GLS is normal or mildly reduced in CP but there are regional variations in LS impairment. Because of the pericardial adhesions, lateral wall LS is often reduced whereas septal LS is usually preserved, resulting in reduced ratio of lateral wall to septal LS [44•, 47]. This ratio has been demonstrated to be highly accurate in differentiating CP from RCM, and even superior to the ratio of medial to lateral e' velocity (areas under the curve 0.91 and 0.76 respectively,  $p = 0.011$ ) [44•]. Furthermore, it has also been shown to correlate with the regional pericardial thickness. The pericardial restraint in CP also results in reduced overall longitudinal displacement of LV base, despite increased annular velocities [29•, 47]. In addition, RV free wall LS is also reduced due to pericardial adhesions [44•]. These abnormalities improve with pericardectomy, though the extent of improvement varies depending on the extent of underlying myocardial dysfunction, etiology of CP, as well as the adequacy of pericardial stripping [29•, 44•, 47].

In addition to septal-lateral regionality, there is variation in LS between LV base and apex as well. Sengupta et al. [29•] demonstrated uniform reduction in LS from base to apex in RCM but impairment of only apical LS in CP. Direct anatomical proximity of epicardial and endocardial fibers in the apical region was postulated as the mechanism responsible for reduced apical LS in CP.

### *Circumferential Shortening and Twist Mechanics*

CP is characterized by marked impairment of short-axis deformation of the left ventricle, which is reflected mainly in reduced LV twist and circumferential strain (CS) [29•, 42, 44•, 47]. Reduction in LV twist is primarily due to impairment of apical LV rotation; basal rotation may or may not be

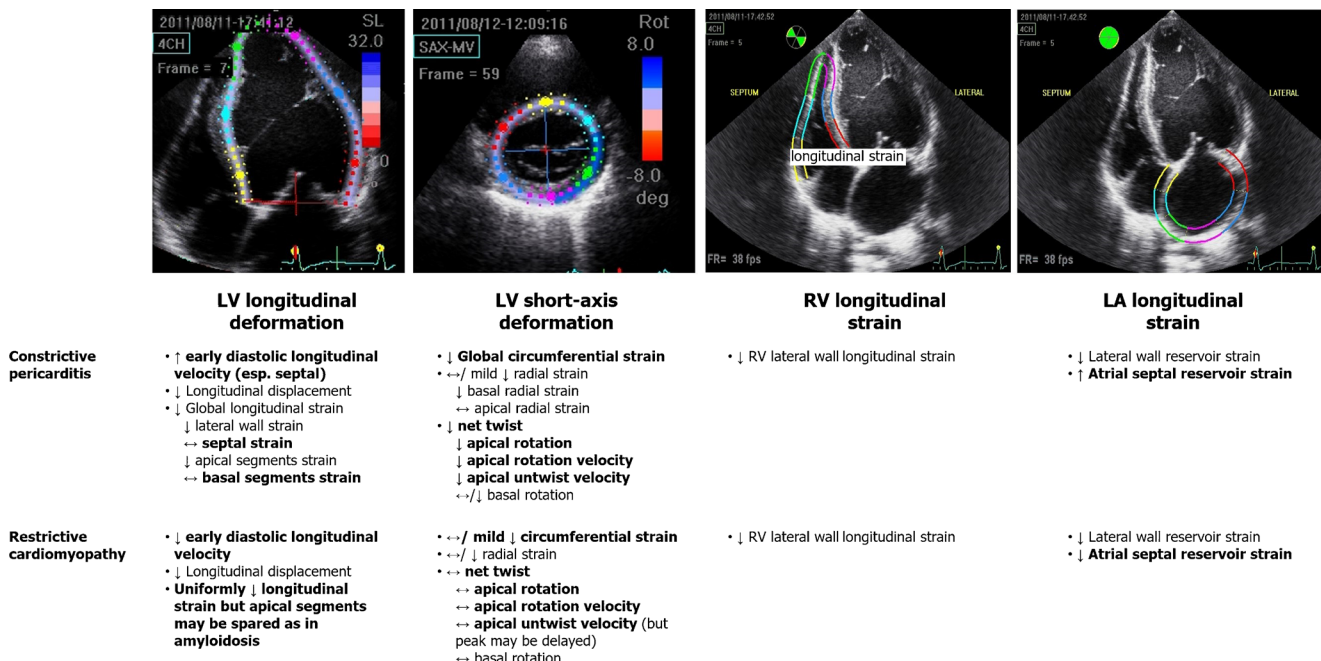


**Fig. 3** Summary of abnormalities in myocardial mechanics in constrictive pericarditis and restrictive cardiomyopathy. The key differentiating features are highlighted in *bold*. *LA* left atrial, *LV* left ventricular, *RV* right ventricular

impaired. The marked impairment of LV short-axis deformation is due to the combined influences of pericardial adhesions as well as subepicardial myocardial layer dysfunction. In comparison, CS is generally preserved in RCM [48].

The effect of CP on RS is less consistent, likely because of variable contribution of epicardial and endocardial fibers to radial thickening. RS, however, is generally reduced in RCM [29•, 44•, 47].

The recovery of myocardial mechanics with treatment of CP varies according to the mode of the treatment [29•, 42, 44•, 49]. Pericardectomy generally leads to incomplete improvement in twist mechanics, mainly because a smooth pericardial surface is essential to facilitate myocardial sliding [29•]. In contrast, complete recovery of LV mechanics has been demonstrated with successful pharmacological management of CP, as in patients with tubercular pericarditis [42].

#### LA Deformation

As with the left ventricle, pericardial adhesions also affect LA deformation. LA free wall total and reservoir strain have been shown to be impaired in CP whereas septal strain values are normal or exaggerated [50, 51]. Pericardectomy tends to restore normal LA mechanics [50, 51].

#### Incremental Value of Myocardial Deformation Imaging for Differentiating CP from RCM

STE permits regional assessment of myocardial deformation which provides for a novel diagnostic tool for CP. As

described above, CP and RCM involve different layers of LV myocardium resulting in disparate changes in myocardial mechanics. STE can discern these abnormalities, providing incremental diagnostic value over conventional echocardiography. For example, Sengupta et al. found that combining mitral  $e'$  with peak early diastolic untwisting velocity could substantially reduce overlap between CP and RCM [29•]. Furthermore, STE demonstrates exaggerated longitudinal septal deformation but impaired lateral wall deformation of both left atrium and left ventricle, which appears to be characteristic of CP [44•, 47, 50, 51]. It has been suggested that the tethering effect of pericardial thickening in CP is often patchy and may spare the annulus [28, 44•], thereby compromising the reliability of annular velocities to differentiate constriction from restriction. Thus, even though regional discordance has been demonstrated in annular velocities also [28], regional LS improves the sensitivity and specificity to diagnose CP as compared to using regional annular velocities alone [44•]. Finally, STE also permits evaluation of the success of pericardectomy.

#### Limitations of STE

The accuracy of STE is dependent on gray-scale image quality which may be suboptimal in many patients with CP due to acoustic shadowing from thickened, calcified pericardium. It is also limited by the problem of through-plane motion, which is particularly more marked for short-axis imaging.

The assessment of the LA function by STE has additional challenges. During transthoracic echocardiography, LA is situated farther from the transducer in apical views. In addition,

the LA myocardium is thinner and brighter than the LV myocardium, with fewer speckle kernels to track. There is also no validation study of STE-based LA strain measurement against sonomicrometry or tagged CMR.

### Role of Machine-Learning Approaches

It is evident from the preceding discussion that no single echocardiographic parameter is robust enough to accurately distinguish between CP and RCM. Accordingly, a cluster of variables need to be combined to achieve an optimum diagnostic accuracy. Welch et al. demonstrated utility of one such approach combining conventional echocardiographic parameters [40], whereas other investigators have demonstrated incremental gain in accuracy by incorporating STE data [29, 44, 48]. However, these approaches have included only a limited number of echocardiographic variables, thereby still under-recognizing the true diagnostic potential of the modality.

Every routine echocardiographic examination generates a wealth of diagnostically useful data and the amount of data generated during each examination has seen an exponential growth with the advent of STE. However, most of this diagnostically relevant information remains unutilized because of the inability of human minds to interpret and assimilate such large, complex datasets, particularly in the busy clinical environments. The advances in computer technology with the development of cognitive computing tools or “artificial intelligence” or “deep machine-learning” offers an exciting solution to meet this challenge.

Machine-learning essentially involves developing algorithms to recognize patterns of abnormalities in a cluster of variables that have the greatest discriminatory ability. Datasets from a large number of patients are used to train the computer algorithms to develop matrices or “fingerprints” that are unique to each specific pathology. Once adequately trained, the computer algorithm can then easily make diagnostic interpretations by matching the pattern of abnormality in the test dataset with those already stored in the memory (Fig. 4) [52]. In this manner, the functioning of a machine-learning approach is akin to that of an experienced clinician or echocardiographer who is able to make instant clinical judgments by recalling extensive, stored knowledge in his/her brain acquired through years of experience.

The use of machine-learning approaches in the field of medicine is increasing rapidly [52, 53, 54]. Sengupta et al. were the first to apply the concept of machine-learning to the complex clinical challenge of differentiating CP from RCM [52]. Using only STE variables, the machine-learning algorithm achieved a high degree of diagnostic accuracy with area under the curve of 89.2%. This was significantly greater than that for mitral e' or GLS (areas under the curve 82.1 and 63.7%, respectively). But more importantly, when the top 15

STE variables were combined with the four conventional echocardiographic variables (mitral e', mitral E/e', ventricular septal thickness, and posterior wall thickness), the area under the curve increased to 96.2%. Such high degree of accuracy could be achieved because the automated algorithm was able to recognize the top 15 STE variables and evaluate their interactions with each other as well as with the 4 most predictive conventional echocardiographic parameters. Such complex, multidimensional analytics is clearly beyond the human capabilities. This study thus demonstrated the potential of automated machine-learning for improving diagnostic accuracy of echocardiographic interpretations. The less-experienced or novice readers are likely to be benefitted the most as the accuracy of a machine-learning algorithm is virtually independent of the “operator expertise”. Further advancements in computer technology are now required to facilitate incorporation of such automated approaches in the routine workflow of the echocardiography labs.

### Cardiac CT

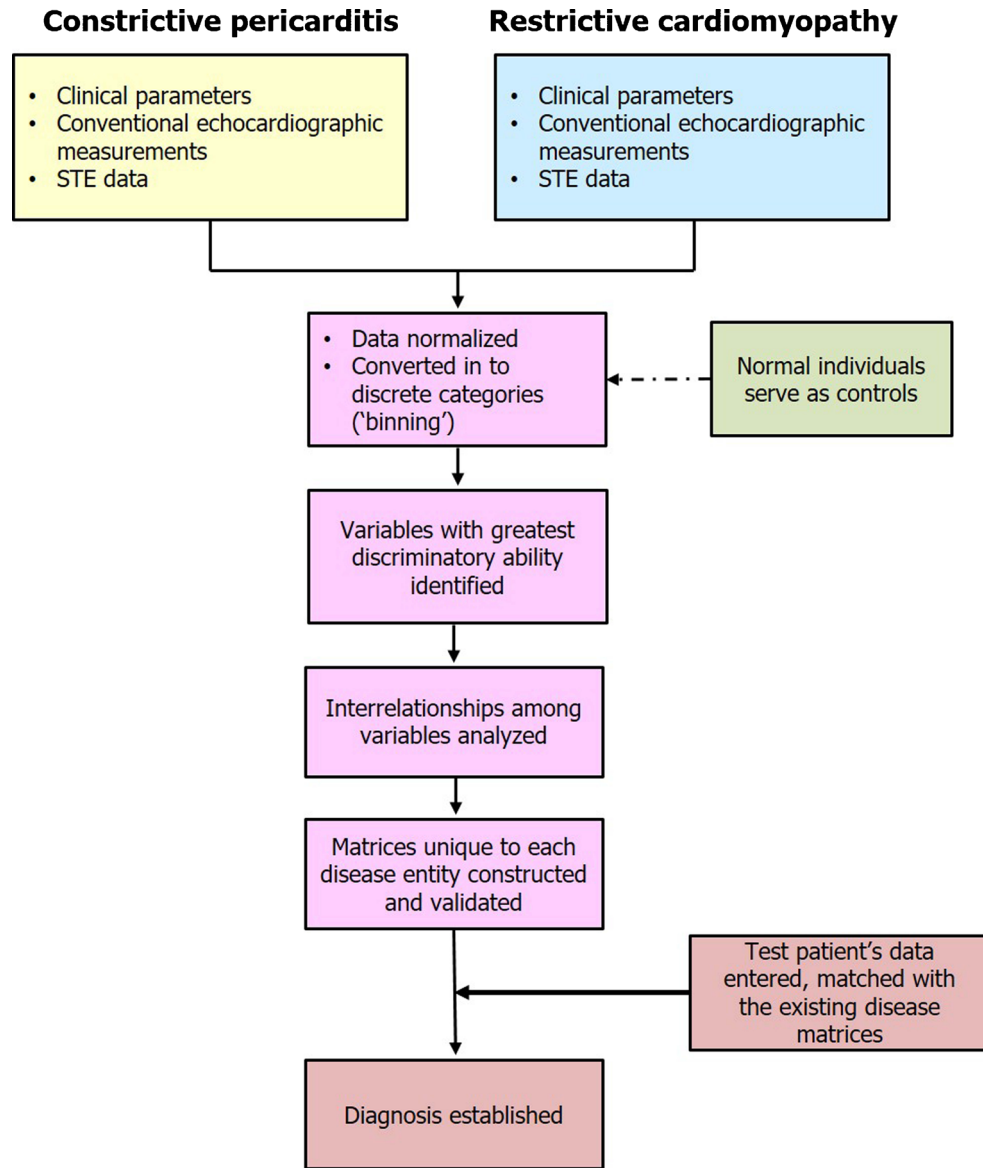
Given its high spatial resolution, CT provides excellent delineation of pericardial anatomy. Normal pericardial thickness on CT is <2 mm [55] and a thickness of >4 mm, in appropriate clinical setting, is highly suggestive of CP [20, 30, 56]. However, it should be noted that a previous study had demonstrated that almost 28% of patients with surgically confirmed CP had normal pericardial thickness on CT [32]. Conversely, pericardial thickening by itself does not confirm CP as many conditions, including uremia, rheumatic heart disease, post-operative state, or exposure to radiation therapy may result in pericardial thickening without necessarily producing constriction. CT is the imaging modality of choice for visualization of pericardial calcification. CT-evidence of pericardial calcification is present in nearly 50% with CP [30].

CT also provides other structural information that serves as corroborative evidence for the constrictive process such as conical shaped ventricles, distortion of pericardial contour, enlarged right atrium, dilatation of inferior vena cava and hepatic veins, pleural effusion, ascites, etc. However, some of these features are seen in RCM as well.

Gated CT imaging, using either prospective triggering or retrospective gating, allows dynamic assessment of cardiac motion and can demonstrate the features of ventricular interdependence [30, 57]. However, retrospective gating is associated with high radiation exposure and is usually not preferred.

Finally, CT also provides useful information for pre-operative planning in patients scheduled to undergo pericardectomy [30]. The location and the extent of pericardial thickening and calcification and the presence and extent of concomitant lung pathology are helpful in surgical

**Fig. 4** Schematic depicting use of machine-learning algorithms for differential diagnosis of constrictive pericarditis and restrictive cardiomyopathy



planning. Additionally, CT coronary angiography may also obviate the need for invasive coronary angiography in many patients.

## CMR

CMR is an excellent modality for the evaluation of CP and RCM. It has high spatial resolution and compared with CT has superior temporal resolution. CMR provides excellent visualization of pericardial thickening and is also able to distinguish between pericardial thickening and small pericardial effusions. A pericardial thickness of >4 mm on CMR has been shown to have 93% diagnostic accuracy for differentiating CP from RCM, and thickness of  $\geq 5\text{--}6$  mm has very high

specificity for CP [58, 59]. However, CMR is inferior to CT for assessment of pericardial calcification.

The use of certain specific CMR sequences such as short-tau inversion recovery and/or gadolinium contrast permits assessment of pericardial edema and inflammation [2<sup>••</sup>, 3<sup>••</sup>, 60–62]. The presence of pericardial inflammation not only supports a diagnosis of evolving constriction, but also indicates reversibility of pericarditis with appropriate medical treatment [61, 62]. Furthermore, quantitative assessment of pericardial late gadolinium enhancement LGE in patients with CP treated with anti-inflammatory therapy can provide additional prognostic value when combined with other clinical features and Westergren sedimentation rates [63]. Although late gadolinium enhancement (LGE) may be seen in CP, it is confined to pericardial region (and adjacent myocardium in cases of myopericarditis), whereas myocardial LGE is common in RCM [2<sup>••</sup>, 64].

An added advantage of CMR is that real-time dynamic imaging is feasible without any concerns about radiation exposure. Respiratory shift in ventricular septal position and relative changes in RV and LV volumes can be easily assessed, permitting accurate diagnosis of CP [65–67]. Further, the use of phase-encoded velocimetry allows measurement of intracardiac flows in a manner analogous to Doppler echocardiography [68].

Tagged cine CMR and tissue-tracking are robust modalities for assessment of myocardial motion and are useful for evaluation of CP. Lack of free sliding motion of the myocardium in relation to the parietal pericardium on tagged cine CMR indicates pericardial adhesions and supports a diagnosis of CP [69, 70]. Further, tagged cine CMR and CMR tissue-tracking or feature-tracking also permit comprehensive analysis of myocardial deformation. A previous study has already demonstrated excellent concordance between STE- and CMR-derived LV myocardial mechanics for differentiating CP from RCM [48].

Lastly, CMR is a unique modality that permits tissue characterization non-invasively, which is very helpful in the evaluation of RCM. Myocardial LGE is seen in nearly one third of all cases of RCM [71]. In certain myocardial diseases, such as amyloidosis, the pattern of myocardial delayed enhancement is quite characteristic and can virtually confirm the etiological diagnosis [72, 73]. Additionally, LGE may also have prognostic value in these conditions [74].

## Conclusions

The differentiation between CP and RCM is crucial but remains challenging. Echocardiography is the preferred modality for this purpose. However, conventional echocardiography alone may not permit accurate diagnostic assessment in all cases. The use of newer algorithms integrating multiple echocardiographic parameters and the incorporation of myocardial mechanics have significantly enhanced the accuracy of echocardiography for this purpose. At the same time, early experience with novel machine-learning approaches has shown great promise in rendering echocardiography much more efficient, accurate, and reproducible. These developments, coupled with the advances in cardiac CT and CMR, have now greatly minimized the need for invasive hemodynamic assessment for differential diagnosis of CP and RCM.

## Compliance with Ethical Standards

**Conflict of Interest** Ahmad Mahmoud, Manish Bansal, and Partho P. Sengupta declare that they have no conflict of interest.

**Human and Animal Rights and Informed Consent** This article does not contain any studies with human or animal subjects performed by any of the authors.

## References

Papers of particular interest, published recently, have been highlighted as:

- Of importance
  - Of major importance
1. •• Dal-Bianco JP, Sengupta PP, Mookadam F, Chandrasekaran K, Tajik AJ, Khandheria BK. Role of echocardiography in the diagnosis of constrictive pericarditis. *J Am Soc Echocardiogr*. 2009;22(1):24–33. doi:[10.1016/j.echo.2008.11.004](https://doi.org/10.1016/j.echo.2008.11.004). **Quiz 103-4. An excellent review article summarizing various conventional echocardiographic criteria, along with their diagnostic accuracies, for distinguishing between restrictive cardiomyopathy and constrictive pericarditis**
  2. •• Geske JB, Anavekar NS, Nishimura RA, Oh JK, Gersh BJ. Differentiation of constriction and restriction: complex cardiovascular hemodynamics. *J Am Coll Cardiol*. 2016;68(21):2329–47. doi:[10.1016/j.jacc.2016.08.050](https://doi.org/10.1016/j.jacc.2016.08.050). **An excellent review article describing pathophysiological differences between restrictive cardiomyopathy and constrictive pericarditis and approach to the differential diagnosis of the two conditions**
  3. •• Klein AL, Abbara S, Agler DA, Appleton CP, Asher CR, Hoit B et al. American Society of Echocardiography clinical recommendations for multimodality cardiovascular imaging of patients with pericardial disease: endorsed by the Society for Cardiovascular Magnetic Resonance and Society of Cardiovascular Computed Tomography. *J Am Soc Echocardiogr*. 2013;26(9):965–1012 e15. doi:[10.1016/j.echo.2013.06.023](https://doi.org/10.1016/j.echo.2013.06.023). **The American Society of Echocardiography guideline for multimodality imaging in pericardial diseases**
  4. • Welch TD, Ling LH, Espinosa RE, Anavekar NS, Wiste HJ, Lahr BD, et al. Echocardiographic diagnosis of constrictive pericarditis: Mayo Clinic criteria. *Circ Cardiovasc Imaging*. 2014;7(3):526–34. **The original study that formed the basis for the Mayo Clinic criteria for differentiating constrictive pericarditis from restrictive cardiomyopathy**
  5. Himelman RB, Lee E, Schiller NB. Septal bounce, vena cava plethora, and pericardial adhesion: informative two-dimensional echocardiographic signs in the diagnosis of pericardial constriction. *J Am Soc Echocardiogr*. 1988;1(5):333–40.
  6. Engel PJ, Fowler NO, Tei CW, Shah PM, Driedger HJ, Shabetai R, et al. M-mode echocardiography in constrictive pericarditis. *J Am Coll Cardiol*. 1985;6(2):471–4.
  7. Candell-Riera J, Garcia del Castillo H, Permanyer-Miralda G, Soler-Soler J. Echocardiographic features of the interventricular septum in chronic constrictive pericarditis. *Circulation*. 1978;57(6):1154–8.
  8. Sengupta PP, Mohan JC, Mehta V, Arora R, Khandheria BK, Pandian NG. Doppler tissue imaging improves assessment of abnormal interventricular septal and posterior wall motion in constrictive pericarditis. *J Am Soc Echocardiogr*. 2005;18(3):226–30. doi:[10.1016/j.echo.2004.11.017](https://doi.org/10.1016/j.echo.2004.11.017).
  9. Oki T, Tabata T, Yamada H, Abe M, Onose Y, Wakatsuki T, et al. Right and left ventricular wall motion velocities as diagnostic indicators of constrictive pericarditis. *Am J Cardiol*. 1998;81(4):465–70.
  10. Tei C, Child JS, Tanaka H, Shah PM. Atrial systolic notch on the interventricular septal echogram: an echocardiographic sign of constrictive pericarditis. *J Am Coll Cardiol*. 1983;1(3):907–12. doi:[10.1016/s0735-1097\(83\)80207-1](https://doi.org/10.1016/s0735-1097(83)80207-1).
  11. Coylewright M, Welch TD, Nishimura RA. Mechanism of septal bounce in constrictive pericarditis: a simultaneous cardiac catheterisation and echocardiographic study. *Heart*. 2013;99(18):1376. doi:[10.1136/heartjnl-2013-304070](https://doi.org/10.1136/heartjnl-2013-304070).

12. Voelkel AG, Pietro DA, Folland ED, Fisher ML, Parisi AF. Echocardiographic features of constrictive pericarditis. *Circulation*. 1978;58(5):871–5.
13. Oh JK, Hatle LK, Seward JB, Danielson GK, Schaff HV, Reeder GS, et al. Diagnostic role of Doppler echocardiography in constrictive pericarditis. *J Am Coll Cardiol*. 1994;23(1):154–62.
14. Hatle LK, Appleton CP, Popp RL. Differentiation of constrictive pericarditis and restrictive cardiomyopathy by Doppler echocardiography. *Circulation*. 1989;79(2):357–70.
15. Rajagopalan N, Garcia MJ, Rodriguez L, Murray RD, Apperson-Hansen C, Stugaard M, et al. Comparison of new Doppler echocardiographic methods to differentiate constrictive pericardial heart disease and restrictive cardiomyopathy. *Am J Cardiol*. 2001;87(1):86–94.
16. Oh JK, Tajik AJ, Appleton CP, Hatle LK, Nishimura RA, Seward JB. Preload reduction to unmask the characteristic Doppler features of constrictive pericarditis. A new observation. *Circulation*. 1997;95(4):796–9.
17. Ha JW, Oh JK, Ommen SR, Ling LH, Tajik AJ. Diagnostic value of mitral annular velocity for constrictive pericarditis in the absence of respiratory variation in mitral inflow velocity. *J Am Soc Echocardiogr*. 2002;15(12):1468–71. doi:10.1067/mje.2002.127452.
18. Cosyns B, Plein S, Nihoyanopoulos P, Smiseth O, Achenbach S, Andrade MJ, et al. European Association of Cardiovascular Imaging (EACVI) position paper: multimodality imaging in pericardial disease. *Eur Heart J Cardiovasc Imaging*. 2015;16(1):12–31. doi:10.1093/eihci/jeu128.
19. Boonyaratavej S, Oh JK, Tajik AJ, Appleton CP, Seward JB. Comparison of mitral inflow and superior vena cava Doppler velocities in chronic obstructive pulmonary disease and constrictive pericarditis. *J Am Coll Cardiol*. 1998;32(7):2043–8.
20. Ha JW, Ommen SR, Tajik AJ, Barnes ME, Ammash NM, Gertz MA, et al. Differentiation of constrictive pericarditis from restrictive cardiomyopathy using mitral annular velocity by tissue Doppler echocardiography. *Am J Cardiol*. 2004;94(3):316–9.
21. Sengupta PP, Mohan JC, Mehta V, Arora R, Pandian NG, Khandheria BK. Accuracy and pitfalls of early diastolic motion of the mitral annulus for diagnosing constrictive pericarditis by tissue Doppler imaging. *Am J Cardiol*. 2004;93(7):886–90. doi:10.1016/j.amjcard.2003.12.029.
22. Choi EY, Ha JW, Kim JM, Ahn JA, Seo HS, Lee JH, et al. Incremental value of combining systolic mitral annular velocity and time difference between mitral inflow and diastolic mitral annular velocity to early diastolic annular velocity for differentiating constrictive pericarditis from restrictive cardiomyopathy. *J Am Soc Echocardiogr*. 2007;20(6):738–43. doi:10.1016/j.echo.2006.11.005.
23. Nagueh SF, Smiseth OA, Appleton CP, Byrd III BF, Dokainish H, Edvardsen T, et al. Recommendations for the evaluation of left ventricular diastolic function by echocardiography: an update from the American Society of Echocardiography and the European Association of Cardiovascular Imaging. *J Am Soc Echocardiogr*. 2016;29(4):277–314. doi:10.1016/j.echo.2016.01.011.
24. Ha JW, Oh JK, Ling LH, Nishimura RA, Seward JB, Tajik AJ. Annulus paradoxus: transmural flow velocity to mitral annular velocity ratio is inversely proportional to pulmonary capillary wedge pressure in patients with constrictive pericarditis. *Circulation*. 2001;104(9):976–8.
25. Klein AL, Dahiya A. Annular velocities in constrictive pericarditis. *J Am Coll Cardiol Img*. 2011;4(6):576.
26. Reuss CS, Wilansky SM, Lester SJ, Lusk JL, Grill DE, Oh JK, et al. Using mitral 'annulus reversus' to diagnose constrictive pericarditis. *Eur J Echocardiogr*. 2009;10(3):372–5. doi:10.1093/ejehocard/jen258.
27. Veress G, Ling LH, Kim KH, Dal-Bianco JP, Schaff HV, Espinosa RE, et al. Mitral and tricuspid annular velocities before and after pericardectomy in patients with constrictive pericarditis. *Circ Cardiovasc Imaging*. 2011;4(4):399–407. doi:10.1161/CIRCIMAGING.110.959619.
28. Choi JH, Choi JO, Ryu DR, Lee SC, Park SW, Choe YH, et al. Mitral and tricuspid annular velocities in constrictive pericarditis and restrictive cardiomyopathy: correlation with pericardial thickness on computed tomography. *JACC Cardiovasc Imaging*. 2011;4(6):567–75. doi:10.1016/j.jcmg.2011.01.018.
29. Sengupta PP, Krishnamoorthy VK, Abhayaratna WP, Korinek J, Belohlavek M, Sundt 3rd TM, et al. Disparate patterns of left ventricular mechanics differentiate constrictive pericarditis from restrictive cardiomyopathy. *JACC Cardiovasc Imaging*. 2008a;1(1):29–38. doi:10.1016/j.jcmg.2007.10.006. **One of the earliest studies to use two-dimensional speckle tracking echocardiography to characterize changes in myocardial mechanics in patients with constrictive pericarditis and restrictive cardiomyopathy**
30. Leitman M, Bachner-Hinenzon N, Adam D, Fuchs T, Theodorovich N, Peleg E, et al. Speckle tracking imaging in acute inflammatory pericardial diseases. *Echocardiography*. 2011;28(5):548–55. doi:10.1111/j.1540-8175.2010.01371.x.
31. Ling LH, Oh JK, Tei C, Click RL, Breen JF, Seward JB, et al. Pericardial thickness measured with transesophageal echocardiography: feasibility and potential clinical usefulness. *J Am Coll Cardiol*. 1997;29(6):1317–23.
32. Talreja DR, Edwards WD, Danielson GK, Schaff HV, Tajik AJ, Tazelaar HD, et al. Constrictive pericarditis in 26 patients with histologically normal pericardial thickness. *Circulation*. 2003;108(15):1852–7. doi:10.1161/01.CIR.0000087606.18453.FD.
33. Garcia MJ. Constrictive pericarditis versus restrictive cardiomyopathy? *J Am Coll Cardiol*. 2016;67(17):2061–76. doi:10.1016/j.jacc.2016.01.076.
34. Madeira M, Teixeira R, Costa M, Goncalves L, Klein AL. Two-dimensional speckle tracking cardiac mechanics and constrictive pericarditis: systematic review. *Echocardiography*. 2016;33(10):1589–99. doi:10.1111/echo.13293. **An excellent review article describing the role of speckle tracking echocardiography in the evaluation of constrictive pericarditis**
35. Sengupta PP, Korinek J, Belohlavek M, Narula J, Vannan MA, Jahangir A, et al. Left ventricular structure and function: basic science for cardiac imaging. *J Am Coll Cardiol*. 2006;48(10):1988–2001. doi:10.1016/j.jacc.2006.08.030.
36. Sengupta PP, Tajik AJ, Chandrasekaran K, Khandheria BK. Twist mechanics of the left ventricle: principles and application. *JACC Cardiovasc Imaging*. 2008b;1(3):366–76. doi:10.1016/j.jcmg.2008.02.006.
37. Sengupta PP, Khandheria BK, Narula J. Twist and untwist mechanics of the left ventricle. *Heart Fail Clin*. 2008c;4(3):315–24. doi:10.1016/j.hfc.2008.03.001.
38. Sengupta PP, Krishnamoorthy VK, Korinek J, Narula J, Vannan MA, Lester SJ, et al. Left ventricular form and function revisited: applied translational science to cardiovascular ultrasound imaging. *J Am Soc Echocardiogr*. 2007;20(5):539–51.
39. Geyer H, Caracciolo G, Abe H, Wilansky S, Carerj S, Gentile F, et al. Assessment of myocardial mechanics using speckle tracking echocardiography: fundamentals and clinical applications. *J Am Soc Echocardiogr*. 2010;23(4):351–69. **quiz 453–5** doi:10.1016/j.echo.2010.02.015.
40. Omar AM, Bansal M, Sengupta PP. Advances in echocardiographic imaging in heart failure with reduced and preserved ejection fraction. *Circ Res*. 2016;119(2):357–74. doi:10.1161/CIRCRESAHA.116.309128.

41. Claus P, Omar AM, Pedrizzetti G, Sengupta PP, Nagel E. Tissue tracking technology for assessing cardiac mechanics: principles, normal values, and clinical applications. *JACC Cardiovasc Imaging*. 2015;8(12):1444–60. doi:[10.1016/j.jcmg.2015.11.001](https://doi.org/10.1016/j.jcmg.2015.11.001).
42. Bansal M, Mehrotra R, Kasliwal RR. Loss of left ventricular torsion as the predominant mechanism of left ventricular systolic dysfunction in a patient with tubercular cardiomyopathy. *Echocardiography*. 2012;29(9):E221–5. doi:[10.1111/j.1540-8175.2012.01768.x](https://doi.org/10.1111/j.1540-8175.2012.01768.x).
43. Garcia MJ, Rodriguez L, Ares M, Griffin BP, Thomas JD, Klein AL. Differentiation of constrictive pericarditis from restrictive cardiomyopathy: assessment of left ventricular diastolic velocities in longitudinal axis by Doppler tissue imaging. *J Am Coll Cardiol*. 1996;27(1):108–14. doi:[10.1016/0735-1097\(95\)00434-3](https://doi.org/10.1016/0735-1097(95)00434-3).
44. Kusunose K, Dahiya A, Popovic ZB, Motoki H, Alraies MC, Zurick AO, et al. Biventricular mechanics in constrictive pericarditis comparison with restrictive cardiomyopathy and impact of pericardectomy. *Circ Cardiovasc Imaging*. 2013;6(3):399–406. doi:[10.1161/CIRCIMAGING.112.000078](https://doi.org/10.1161/CIRCIMAGING.112.000078). **Another important study to describe changes in myocardial mechanics in patients with constrictive pericarditis and restrictive cardiomyopathy and the impact of pericardectomy on myocardial mechanics**
45. Phelan D, Collier P, Thavendiranathan P, Popovic ZB, Hanna M, Plana JC, et al. Relative apical sparing of longitudinal strain using two-dimensional speckle-tracking echocardiography is both sensitive and specific for the diagnosis of cardiac amyloidosis. *Heart*. 2012;98(19):1442–8. doi:[10.1136/heartjnl-2012-302353](https://doi.org/10.1136/heartjnl-2012-302353).
46. Baccouche H, Maunz M, Beck T, Gaa E, Banzhaf M, Knayer U, et al. Differentiating cardiac amyloidosis and hypertrophic cardiomyopathy by use of three-dimensional speckle tracking echocardiography. *Echocardiography*. 2012;29(6):668–77. doi:[10.1111/j.1540-8175.2012.01680.x](https://doi.org/10.1111/j.1540-8175.2012.01680.x).
47. Negishi K, Popovic ZB, Negishi T, Motoki H, Alraies MC, Chirakarnjanakorn S, et al. Pericardectomy is associated with improvement in longitudinal displacement of left ventricular free wall due to increased counterclockwise septal-to-lateral rotational displacement. *J Am Soc Echocardiogr*. 2015;28(10):1204–13.e2. doi:[10.1016/j.echo.2015.05.011](https://doi.org/10.1016/j.echo.2015.05.011).
48. Amaki M, Savino J, Ain DL, Sanz J, Pedrizzetti G, Kulkarni H, et al. Diagnostic concordance of echocardiography and cardiac magnetic resonance-based tissue tracking for differentiating constrictive pericarditis from restrictive cardiomyopathy. *Circ Cardiovasc Imaging*. 2014;7(5):819–27. doi:[10.1161/CIRCIMAGING.114.002103](https://doi.org/10.1161/CIRCIMAGING.114.002103).
49. Vogel JH, Horgan JA, Strahl CL. Left ventricular dysfunction in chronic constrictive pericarditis. *Chest*. 1971;59(5):484–92.
50. Motoki H, Alraies MC, Dahiya A, Saraiva RM, Hanna M, Marwick TH, et al. Changes in left atrial mechanics following pericardectomy for pericardial constriction. *J Am Soc Echocardiogr*. 2013;26(6):640–8. doi:[10.1016/j.echo.2013.02.014](https://doi.org/10.1016/j.echo.2013.02.014).
51. Liu S, Ma C, Ren W, Zhang J, Li N, Yang J, et al. Regional left atrial function differentiation in patients with constrictive pericarditis and restrictive cardiomyopathy: a study using speckle tracking echocardiography. *Int J Cardiovasc Imaging*. 2015;31(8):1529–36. doi:[10.1007/s10554-015-0726-7](https://doi.org/10.1007/s10554-015-0726-7).
52. Sengupta PP, Huang YM, Bansal M, Ashrafi A, Fisher M, Shameer K, et al. Cognitive machine-learning algorithm for cardiac imaging: a pilot study for differentiating constrictive pericarditis from restrictive cardiomyopathy. *Circ Cardiovasc Imaging*. 2016;9(6). doi:[10.1161/CIRCIMAGING.115.004330](https://doi.org/10.1161/CIRCIMAGING.115.004330). **The first study to evaluate the role of automated machine-learning algorithms in differential diagnosis of constrictive pericarditis and restrictive cardiomyopathy**.
53. Narula S, Shameer K, Salem Omar AM, Dudley JT, Sengupta PP. Machine-learning algorithms to automate morphological and functional assessments in 2D echocardiography. *J Am Coll Cardiol*. 2016;68(21):2287–95. doi:[10.1016/j.jacc.2016.08.062](https://doi.org/10.1016/j.jacc.2016.08.062).
54. Dilsizian SE, Siegel EL. Artificial intelligence in medicine and cardiac imaging: harnessing big data and advanced computing to provide personalized medical diagnosis and treatment. *Curr Cardiol Rep*. 2014;16(1):441. doi:[10.1007/s11886-013-0441-8](https://doi.org/10.1007/s11886-013-0441-8).
55. Bull RK, Edwards PD, Dixon AK. CT dimensions of the normal pericardium. *Br J Radiol*. 1998;71(849):923–5. doi:[10.1259/bjr.71.849.10195005](https://doi.org/10.1259/bjr.71.849.10195005).
56. Verhaert D, Gabriel RS, Johnston D, Lytle BW, Desai MY, Klein AL. The role of multimodality imaging in the management of pericardial disease. *Circ Cardiovasc Imaging*. 2010;3(3):333–43. doi:[10.1161/CIRCIMAGING.109.921791](https://doi.org/10.1161/CIRCIMAGING.109.921791).
57. Gherdin E, Lessick J, Litmanovich D, Ofer A, Elhasid R, Lorber A, et al. Septal bounce in constrictive pericarditis. Diagnosis and dynamic evaluation with multidetector CT. *J Comput Assist Tomogr*. 2004;28(5):676–8.
58. Soulard RL, Stark DD, Higgins CB. Magnetic resonance imaging of constrictive pericardial disease. *Am J Cardiol*. 1985;55(4):480–4.
59. Masui T, Finck S, Higgins CB. Constrictive pericarditis and restrictive cardiomyopathy: evaluation with MR imaging. *Radiology*. 1992;182(2):369–73. doi:[10.1148/radiology.182.2.1732952](https://doi.org/10.1148/radiology.182.2.1732952).
60. Alter P, Figiel JH, Rupp TP, Bachmann GF, Maisch B, Rominger MB. MR, CT, and PET imaging in pericardial disease. *Heart Fail Rev*. 2013;18(3):289–306. doi:[10.1007/s10741-012-9309-z](https://doi.org/10.1007/s10741-012-9309-z).
61. Zurick AO, Bolen MA, Kwon DH, Tan CD, Popovic ZB, Rajeswaran J, et al. Pericardial delayed hyperenhancement with CMR imaging in patients with constrictive pericarditis undergoing surgical pericardectomy: a case series with histopathological correlation. *JACC Cardiovasc Imaging*. 2011;4(11):1180–91. doi:[10.1016/j.jcmg.2011.08.011](https://doi.org/10.1016/j.jcmg.2011.08.011).
62. Feng D, Glockner J, Kim K, Martinez M, Syed IS, Araoz P, et al. Cardiac magnetic resonance imaging pericardial late gadolinium enhancement and elevated inflammatory markers can predict the reversibility of constrictive pericarditis after antiinflammatory medical therapy: a pilot study. *Circulation*. 2011;124(17):1830–7. doi:[10.1161/CIRCULATIONAHA.111.026070](https://doi.org/10.1161/CIRCULATIONAHA.111.026070).
63. Cremer PC, Kumar A, Kontzias A, Tan CD, Rodriguez ER, Imazio M, et al. Complicated pericarditis: understanding risk factors and pathophysiology to inform imaging and treatment. *J Am Coll Cardiol*. 2016;68(21):2311–28. doi:[10.1016/j.jacc.2016.07.785](https://doi.org/10.1016/j.jacc.2016.07.785).
64. Cremer PC, Tariq MU, Karwa A, Alraies MC, Benatti R, Schuster A, et al. Quantitative assessment of pericardial delayed hyperenhancement predicts clinical improvement in patients with constrictive pericarditis treated with anti-inflammatory therapy. *Circ Cardiovasc Imaging*. 2015;8(5). doi:[10.1161/CIRCIMAGING.114](https://doi.org/10.1161/CIRCIMAGING.114).
65. Giorgi B, Mollet NR, Dymarkowski S, Rademakers FE, Bogaert J. Clinically suspected constrictive pericarditis: MR imaging assessment of ventricular septal motion and configuration in patients and healthy subjects. *Radiology*. 2003;228(2):417–24.
66. Anavekar NS, Wong BF, Foley TA, Bishu K, Kolipaka A, Koo CW, et al. Index of biventricular interdependence calculated using cardiac MRI: a proof of concept study in patients with and without constrictive pericarditis. *Int J Cardiovasc Imaging*. 2013;29(2):363–9. doi:[10.1007/s10554-012-0101-x](https://doi.org/10.1007/s10554-012-0101-x).
67. Francone M, Dymarkowski S, Kalantzi M, Rademakers FE, Bogaert J. Assessment of ventricular coupling with real-time cine MRI and its value to differentiate constrictive pericarditis from restrictive cardiomyopathy. *Eur Radiol*. 2006;16(4):944–51.
68. Thavendiranathan P, Verhaert D, Walls MC, Bender JA, Rajagopalan S, Chung YC, et al. Simultaneous right and left heart real-time, free-breathing CMR flow quantification identifies constrictive physiology. *JACC Cardiovasc Imaging*. 2012;5(1):15–24. doi:[10.1016/j.jcmg.2011.07.010](https://doi.org/10.1016/j.jcmg.2011.07.010).
69. Kojima S, Yamada N, Goto Y. Diagnosis of constrictive pericarditis by tagged cine magnetic resonance imaging. *N Engl J Med*. 1999;341(5):373–4. doi:[10.1056/NEJM199907293410515](https://doi.org/10.1056/NEJM199907293410515).

70. Bogabathina H, Biederman RW. Lack of slippage by cardiovascular magnetic resonance imaging is sine qua non for constrictive pericarditis. *Circulation*. 2011;123(16):e418–9. doi:[10.1161/CIRCULATIONAHA.110.955229](https://doi.org/10.1161/CIRCULATIONAHA.110.955229).
71. Cheng H, Zhao S, Jiang S, Lu M, Yan C, Ling J, et al. The relative atrial volume ratio and late gadolinium enhancement provide additive information to differentiate constrictive pericarditis from restrictive cardiomyopathy. *J Cardiovasc Magn Reson*. 2011;13:15. doi:[10.1186/1532-429X-13-15](https://doi.org/10.1186/1532-429X-13-15).
72. Syed IS, Glockner JF, Feng D, Araoz PA, Martinez MW, Edwards WD, et al. Role of cardiac magnetic resonance imaging in the detection of cardiac amyloidosis. *JACC Cardiovasc Imaging*. 2010;3(2):155–64. doi:[10.1016/j.jcmg.2009.09.023](https://doi.org/10.1016/j.jcmg.2009.09.023).
73. Muehlberg F, Toepper A, Fritsch S, Prothmann M, Schulz-Menger J. Magnetic resonance imaging applications on infiltrative cardiomyopathies. *J Thorac Imaging*. 2016;31(6):336–47. doi:[10.1097/RTI.0000000000000199](https://doi.org/10.1097/RTI.0000000000000199).
74. Boynton SJ, Geske JB, Dispensieri A, Syed IS, Hanson TJ, Grogan M, et al. LGE provides incremental prognostic information over serum biomarkers in AL cardiac amyloidosis. *JACC Cardiovasc Imaging*. 2016;9(6):680–6. doi:[10.1016/j.jcmg.2015.10.027](https://doi.org/10.1016/j.jcmg.2015.10.027).